

## Neurobiological Changes of Schizotypy: Evidence From Both Volume-Based Morphometric Analysis and Resting-State Functional Connectivity

Yi Wang<sup>1,7</sup>, Chao Yan<sup>2,7</sup>, Da-zhi Yin<sup>3</sup>, Ming-xia Fan<sup>3</sup>, Eric F. C. Cheung<sup>4</sup>, Christos Pantelis<sup>5</sup>, and Raymond C. K. Chan<sup>\*1,6</sup>

<sup>1</sup>Neuropsychology and Applied Cognitive Neuroscience Laboratory, Key Laboratory of Mental Health, Institute of Psychology, Chinese Academy of Sciences, Beijing, China; <sup>2</sup>Shanghai Key Laboratory of Brain Functional Genomics (MOE & STCSM), School of Psychology and Cognitive Science, East China Normal University, Shanghai, China; <sup>3</sup>Shanghai Key Laboratory of MRI, East China Normal University, Shanghai, China; <sup>4</sup>Castle Peak Hospital, Hong Kong Special Administrative Region, China; <sup>5</sup>Melbourne Neuropsychiatry Centre, Department of Psychiatry, University of Melbourne and Melbourne Health, Melbourne, Australia; <sup>6</sup>Magnetic Resonance Imaging Centre, Institute of Psychology, Chinese Academy of Sciences, Beijing, China

<sup>7</sup>These authors contributed equally to the study.

\*To whom correspondence should be addressed; Raymond Chan, Institute of Psychology, Chinese Academy of Sciences, 16 Lincui Road, Beijing 100101, China; tel/fax: (86)-10-64877349; e-mail: [rckchan@psych.ac.cn](mailto:rckchan@psych.ac.cn)

The current study sought to examine the underlying brain changes in individuals with high schizotypy by integrating networks derived from brain structural and functional imaging. Individuals with high schizotypy ( $n = 35$ ) and low schizotypy ( $n = 34$ ) controls were screened using the Schizotypal Personality Questionnaire and underwent brain structural and resting-state functional magnetic resonance imaging on a 3T scanner. Voxel-based morphometric analysis and graph theory-based functional network analysis were conducted. Individuals with high schizotypy showed reduced gray matter (GM) density in the insula and the dorsolateral prefrontal gyrus. The graph theoretical analysis showed that individuals with high schizotypy showed similar global properties in their functional networks as low schizotypy individuals. Several hubs of the functional network were identified in both groups, including the insula, the lingual gyrus, the postcentral gyrus, and the rolandic operculum. More hubs in the frontal lobe and fewer hubs in the occipital lobe were identified in individuals with high schizotypy. By comparing the functional connectivity between clusters with abnormal GM density and the whole brain, individuals with high schizotypy showed weaker functional connectivity between the left insula and the putamen, but stronger connectivity between the cerebellum and the medial frontal gyrus. Taken together, our findings suggest that individuals with high schizotypy present changes in terms of GM and resting-state functional connectivity, especially in the frontal lobe.

**Key words:** schizotypy/voxel-based morphometry/graph theory/functional connectivity/insula

### Introduction

Recent population-based studies have suggested that psychotic-like experiences exist as a part of continuum in the general population.<sup>1</sup> Schizotypy is a set of enduring traits and phenotypic expression of the familial-genetic liability to schizophrenia.<sup>2</sup> The importance of schizotypy in understanding the psychopathology of schizophrenia has recently been emphasized because empirical evidence suggests that individuals with high schizotypy and patients with established schizophrenia show similar but attenuated dysfunctions in cognition and perception,<sup>3</sup> emotional processing,<sup>4</sup> as well as brain structural and functional abnormalities.<sup>1,3</sup>

However, the extant literature has been complicated by different definitions of schizotypy. Conventionally, there are 2 methods used to study this target population, namely the clinical diagnosis and the psychometric approach. The former adopts the Diagnostic and Statistical Manual of Mental Disorders, Fourth Edition (DSM-IV-TR)<sup>5</sup> system to identify either personality-disordered patients who seem to exhibit attenuated schizophrenic symptoms or biological relatives of patients with schizophrenia who exhibit subtle schizophrenia-like psychopathology.<sup>6</sup> The latter approach is based upon psychometrically validated checklists, such as the Schizotypal Personality Questionnaire (SPQ)<sup>7</sup> and the Wisconsin Schizotypy Scales,<sup>8–10</sup> to screen out individuals who show more schizophrenia-like experiences. Compared with healthy controls, individuals with clinically diagnosed schizotypy showed brain abnormalities

similar to patients with schizophrenia,<sup>11</sup> including gray matter (GM) volume reduction at the superior temporal gyrus (STG),<sup>12</sup> the insula and the inferior frontal gyrus,<sup>13</sup> the caudate nucleus,<sup>14</sup> and the fusiform gyrus.<sup>15</sup> Most recently, the largest study to date conducted to examine the brain structures in 54 clinically diagnosed medication-naïve schizotypy individuals using voxel-based morphometry (VBM) showed that men with schizotypy exhibited global and widespread smaller regional GM volumes, particularly in the left STG, frontal, frontolimbic, and parietal regions.<sup>16</sup> Moreover, these changes were significantly associated with negative symptoms.<sup>16</sup>

Although few studies have examined individuals with psychometrically defined schizotypy, the findings indicated structural abnormalities. For example, GM volume reductions in the medial prefrontal, the orbitofrontal, and the temporal cortical regions have been found in individuals with high positive schizotypy,<sup>17</sup> while larger posterior cingulate cortex and precuneus regional volumes have also been found in individuals with psychometric schizotypy as measured by the Community Assessment of Psychic Experiences (CAPE).<sup>18</sup> A diffusion tensor imaging study found significant correlations between fractional anisotropy reduction and higher scores on the cognitive-perceptual factor of the schizotypal traits.<sup>19</sup> Furthermore, significant positive correlations were observed between the cortical thickness of the right dorsolateral prefrontal cortex (dlPFC) and SPQ total scores.<sup>20</sup>

Recently, researchers have suggested that the brain mechanisms underlying schizophrenia reflect dysfunction of brain networks, instead of abnormalities in specific brain regions.<sup>21</sup> Recently, graph-based brain network analysis has contributed to the exploration of the underlying neural mechanisms in patients with mental disorders.<sup>22</sup> Empirical findings have shown that the disrupted small-world properties obtained from resting-state functional imaging in patients with schizophrenia are mainly present in brain regions in the temporal, prefrontal, and parietal lobes.<sup>23</sup> To the best of our knowledge, only one study had examined the associations between resting-state functional networks and schizotypal traits using group-level-independent component analysis. Significant correlations were found between SPQ scores and both visual and auditory networks in adolescents.<sup>24</sup> Little is known about the resting-state functional connectivity in individuals with schizotypy, especially the associations of the abnormal functional connectivity with dimensions of schizotypy.

It is noteworthy that most of the imaging studies of schizotypy were carried out in clinically diagnosed participants, and very few studies have made use of individuals with psychometrically defined schizotypy. As an enduring trait characterized by schizophrenia-like symptoms, the study of psychometrically defined schizotypy plays an equally important role in the understanding

of the course of development of schizophrenia. Most recently a standard terminology of schizotypy has been agreed upon by researchers in this field to capture all the interchangeable terms of schizotypal personality, psychotic-like experiences, and subclinical psychotic experiences.<sup>1</sup> Therefore, we operationally defined individuals with schizotypal personality traits as the traits generally covering these concepts and referred to them as "schizotypy."

The purposes of the current study were to (1) examine if there were any morphometric abnormalities in GM and white matter (WM) between individuals with high and low schizotypy individuals; (2) examine the small-world network properties during resting state in both groups and compare the characteristics of network and nodes between the high and low schizotypy group; and (3) examine if there was any difference in functional connectivity between the high schizotypy and the low schizotypy group at those brain regions where high schizotypy individuals demonstrated structural abnormality. To the best of our knowledge, this is the first study integrating structural analysis and functional network analysis to examine abnormalities in individuals with schizotypy. We hypothesized that compared with low schizotypy, individuals with high schizotypy might have structural and functional abnormalities in the frontal-parietal-temporal region.

## Methods

### Participants

There were 2 groups of participants in our study: individuals with high psychometrically defined schizotypy (the high schizotypy group) and those with low schizotypy (the low schizotypy group). All participants were selected from a large sample pool consisting of 873 college students from Shanghai (age 16–23 years old, mean age = 19.3 years, SD = 1.0; 204 are male) using the SPQ.<sup>7,25</sup> Participants whose total scores on SPQ were above the top 10th percentile were recruited into the high schizotypy group ( $n = 35$ ). We then randomly chose those participants whose SPQ total scores were in the bottom 50% and recruited them into the low schizotypy group ( $n = 34$ ). All participants were right-handed as assessed by the Annett Handedness Scale<sup>26</sup> and free from personal and family history of mental or neurological disorder, as well as drug abuse. The high schizotypy group had a mean age of 19.7 years (SD = 1.1) and consisted of 19 males. The low schizotypy group had a mean age of 20.1 years (SD = 0.9) and consisted of 15 males. IQ scores were estimated using the common sense, arithmetic, similarity, and digit span subtests of the Chinese Version Wechsler Adult Intelligence Scale-Revised.<sup>27</sup> The mean IQ estimates for the high schizotypy and the low schizotypy group were 127.89 (SD = 8.23) and 125.71 (SD = 8.18), respectively. No significant differences were found between the

2 groups on age ( $t = 1.85$ ,  $P > .05$ ), gender ( $\chi^2 = 0.71$ ,  $P > .10$ ), and IQ estimates ( $t = 1.10$ ,  $P > .10$ ). The current study was approved by the Ethics Committee of the Institute of Psychology, Chinese Academy of Sciences. Written informed consents were obtained from all participants prior to the study.

### *Measurements*

SPQ<sup>7,25</sup> is a self-report scale modeled on the DSM-III-R criteria for schizotypal personality disorder and consists of 74 items. It has been used to screen for psychometrically defined schizotypal personality disorder in the general population. The 3-factor structure of the SPQ has been validated and includes the cognitive-perceptual, the interpersonal, and the disorganized factors.<sup>25</sup> Consistent with previous study,<sup>25</sup> the reliability of the Chinese version of the SPQ was 0.89 for the whole scale and 0.78–0.85 for its 3 subscales.

### *Images Acquisition and Preprocessing*

All magnetic resonance imaging (MRI) scans were acquired on a Siemens Trio 3T MR scanner at the MRI center of the East China Normal University. For each participant, T1-weighted images were acquired using a 3D magnetic prepared rapid gradient echo pulse sequence, with slice thickness = 1 mm, echo time (TE) = 2.34 ms, repetition time (TR) = 2530 ms, flip angle = 7°, matrix size = 256 × 256 mm, 192 slices in sagittal plane, field of view (FOV) = 256 mm, voxel size = 1 × 1 × 1 mm. Scans were screened by a radiologist to exclude any incidental clinical abnormalities before further analysis. Preprocessing was performed using diffeomorphic anatomical registration through exponentiated Lie algebra (DARTEL) VBM embedded in SPM8 software package (<http://www.fil.ion.ucl.ac.uk/spm/>; accessed December 5, 2015).<sup>28</sup> T1-weighted structural image of each participant was segmented to identify different brain tissues including GM, WM, and cerebrospinal fluid (CSF). Each participant's GM and WM map was transformed to the customized template space and then to Montreal Neurological Institute (MNI) standard template. The warped GM and WM images were modulated by Jacobian determinants to obtain the GM and WM volume. The modulated GM images were written with an isotropic voxel resolution of 1 × 1 × 1 mm<sup>3</sup>. Finally, these images were smoothed with full width at half maximum kernel of 8 mm.

Resting-state functional MRI (fMRI) data were acquired using a T2-weighted echo-planar imaging (EPI) sequence; 200 whole-brain volumes were collected with slice thickness = 3.5 mm, TE = 30 ms, TR = 2500 ms, flip angle = 90°, matrix size = 64 × 64, 42 slices in coronal plane, FOV = 200 mm, voxel size = 3.1 × 3.1 × 3.5 mm, bandwidth = 2520 Hz/Px. Participants were asked to rest in the scanner with their eyes closed and do not fall to sleep during the acquisition. Preprocessing was

performed using Data Processing Assistant for Resting-State fMRI software<sup>29</sup> based on SPM. The first 10 volumes were removed for signal equilibrium and exclusion of participants' adaptation to the scanning noise. The time differences between slices and interscan head motions were corrected. The head motion parameters of all the participants in the current study are less than 3 mm for translations and 3° for rotations. Coregistration, segmentation, and writing normalization were conducted using unified segmentation on their own T1 image. The fMRI images were further spatially normalized to the MNI EPI template and re-sliced to 3 mm cubic voxels. Finally, temporal band-pass filtering (0.01 <  $f$  < 0.08 Hz) was performed. The nuisance covariates, including head motion parameters, global mean signal, WM signal, and CSF signal were regressed out.

### *Construction of Brain Functional Networks*

Node and edge are 2 key components for construction of a network. In the present study, using the Anatomical Automatic Labeling template,<sup>30</sup> the registered fMRI data were parceled into 90 regions (45 in each hemisphere), which represent the nodes of brain network in our study. For each participant, the time series of each region was calculated by averaging the fMRI time series of all voxels within that region. The Pearson correlation coefficients between the time series of each pair of regions were calculated and generated a 90 × 90 matrix for each participant. Each matrix was then changed into a binarized matrix with fixed sparsity (defined as the total number of edges in a network divided by the maximum possible number of edges) as threshold. In the present study, we repeated this thresholding process using a wide range of sparsity, from 10% to 40%, at the interval of 0.01. Hence, at each sparsity level, we obtained one binarized matrix for each participant, which were used in the graph-based analysis.

### *Graph Theoretical Analysis*

Small-world parameters, including clustering coefficient ( $C_p$ ) and shortest path length ( $L_p$ ), were adopted to describe the network properties.  $C_p$  represents the number of connections that exist between the nearest neighbors of a node as a proportion of the maximum number of possible connections.<sup>22</sup>  $L_p$  is the minimum number of edges that must be traversed to go from one node to another.<sup>22</sup> Compared with random networks, small-world networks should have higher clustering coefficients and similar path lengths. Through comparing the  $C_p$  and  $L_p$  of the real network and random network, 2 indices could be obtained to describe the small-world properties: normalized clustering coefficient ( $\gamma$ ) and normalized shortest path length ( $\lambda$ ). Efficiency of the network was described using global and local efficiency parameters. Global efficiency ( $E_{\text{glob}}$ ) is defined by the inverse of the harmonic mean of the minimum absolute path length between each pair of

nodes, and local efficiency ( $E_{loc}$ ) indicates how well each subgraph exchanges information when the index node is eliminated.<sup>31</sup> Nodal characteristic was described by nodal degree ( $D_{nod}$ ) in our study, which is the number of connections that link the node to the rest of the network.<sup>22</sup> The small-world parameters, global and local efficiency, and nodal degree were calculated using Graph-theoRETical Network Analysis toolkit (GRETNA, <http://www.nitrc.org/projects/gretna/>; accessed December 5, 2015).

### Statistical Analysis

**Group Comparison on GM and WM Density.** Statistical differences in GM and WM volumes between the high schizotypy and low schizotypy groups were tested in SPM8 using the 2 sample *t* test model controlling for age, gender, and IQ. Proportional scaling of the total intracranial volume was used to adjust for the global effects. We used absolute masking with a threshold of 0.2 to avoid any possible overlapping edge effect between the GM and WM. The statistical threshold was set at  $P < .05$  using the AlphaSim correction for multiple comparisons (GM: with a threshold of  $P < .001$  and a minimum cluster size of 521 voxels; WM: with a threshold of  $P < .001$  and a minimum cluster size of 457 voxels).

**Group Comparison on Network and Nodal Characteristics.** To compare the characteristics of the resting-state functional network between the high and the low schizotypy groups, we compared the area under the curve (AUC) of each parameter covering the whole range of sparsity, including the AUC of  $C_p$ ,  $L_p$ ,  $E_{glob}$ , and  $E_{loc}$ . Nonparametric permutation tests (threshold was set at  $P < .05$ , uncorrected, permuted 10 000 times) were conducted with age and gender as covariates. In order to examine the group differences on  $C_p$ ,  $L_p$ ,  $E_{glob}$ , and  $E_{loc}$  at each sparsity level, we conducted the MANOVA in SPSS with age and gender as covariates. The threshold was set at  $P < .05$ .

On the nodal level, to identify hub regions, we calculated the normalized nodal degree for each node in the high schizotypy and the low schizotypy group, respectively. The node was identified as a hub if its normalized nodal degree was higher than the sum of the mean and SD of all nodes of the network, following the same method used in a previous study.<sup>32</sup> If any hubs were identified inconsistently between 2 groups, further group comparisons on the mean nodal degree were conducted with age and gender as covariates and the threshold was set at  $P < .05$ .

**Functional Connectivity of Brain Regions With Abnormal GM Density.** To examine the functional connectivity of those regions, which showed abnormal density in the VBM analysis, we defined regions of interest (ROI) using MarsBar toolbox v0.43<sup>33</sup> according to statistical maps

generated by SPM group comparisons. These ROI maps were then re-sliced to match the functional images and used to calculate the time series correlations to the other voxels of the whole brain using a toolkit for Resting-State fMRI analysis (REST).<sup>34</sup> The correlation maps were then transformed to Fisher *z*-maps and put into 2 sample *t* tests using SPM software implemented in Matlab, with age and gender as covariates in the general linear model. The threshold was set at  $P < .05$  with AlphaSim correction for multiple comparisons ( $P < .001$  at voxel level, with a cluster  $>25$  voxels deemed to be significant).

**Correlations Between Brain Structural/Functional Changes and the SPQ Scores.** Finally, to explore the associations between the brain structural and functional changes and the SPQ scores, partial correlation analyses were conducted. On brain structural changes, we extracted the GM density of the 4 significant clusters from the results of VBM analysis (including the insula, the dlPFC, the declive of the cerebellum in the left hemisphere, the right middle temporal gyrus [MTG]). On the brain functional changes, we adopted the AUC of network parameters ( $C_p$  and  $E_{loc}$ ), as well as the mean degrees of the hubs that showed significant group differences between 2 groups (including 11 ROIs, listed in **table 2** in bold). The partial correlations were calculated in high schizotypy group controlled for age and gender using SPSS. The threshold was set at  $P < .05$ , uncorrected.

## Results

### VBM Abnormalities

As summarized in **table 1**, it was found that individuals with high schizotypy showed GM density reduction in the dlPFC (Brodmann area [BA] 8) and the insula (BA 13) of the left hemisphere but enhanced GM density in the right posterior MTG (pMTG, BA 39) and the left declive. No significant difference was found between individuals with high and low schizotypy in terms of the density of WM. **Figure 1** shows the clusters with significant GM abnormalities in the high schizotypy group.

### Small-World Properties and Group Comparison on Network Properties

As **figure 2** shows, over the range of sparsity from 10% to 40%, the normalized clustering coefficients ( $\gamma$ ) were larger than 1 and the normalized shortest path lengths ( $\lambda$ ) were close to 1 in both the high schizotypy and the low schizotypy groups. Hence, the functional networks of both groups in our study presented similar small-world properties. The results of permutation tests showed that the high schizotypy group showed significant differences from the low schizotypy group on  $C_p$  ( $P = .033$ ) and  $E_{loc}$  ( $P = .006$ ). No difference was found on shortest path length and global efficiency of the network (see **figure 3**).

**Table 1.** Differences on Gray Matter Density Between the High Schizotypy and Low Schizotypy Group

Contrast	Cluster Size	x	y	z	T	Z	Brain Region	Hemi	BA
LS > HS	714	-32	24	40	4.27	3.99	dIPFC	Left	8
	1258	-34	17	-2	4.03	3.79	Insula	Left	13
		-39	12	13	3.29	3.15			
HS > LS	1468	35	-61	29	4.33	4.04	pMTG	Right	39
	638	-13	-82	-18	3.69	3.5	Declive	Left	

Note: Threshold at  $P < .05$ , AlphaSim corrected. dIPFC, dorsolateral prefrontal cortex; Hemi, hemisphere; HS, high schizotypy; LS, low schizotypy; pMTG, posterior middle temporal gyrus.

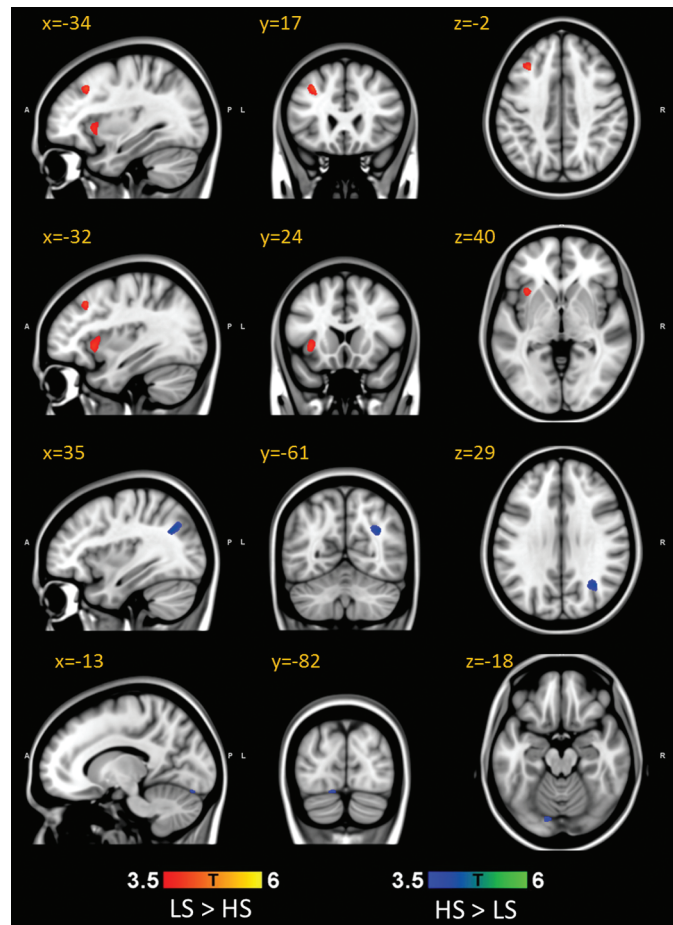


**Fig. 1.** The significant clusters showed gray matter density reduction and enlargement in the high schizotypy group. These clusters include dorsolateral prefrontal cortex, insula, posterior middle temporal gyrus, and cerebellum (declive). HS: high schizotypy; LS: low schizotypy. L: left; R: right. The statistical threshold was set at  $P < .05$  using the AlphaSim correction for multiple comparisons.

#### Group Comparison on Nodal Degree and Hubs Identified

We further identified the hubs using nodal degree as index. As **Table 2** shows, several hub regions were identified consistently in the high schizotypy and the low schizotypy groups, including bilateral insula, the lingual gyrus, the rolandic operculum, the postcentral gyrus, as

well as the anterior cingulate and the paracingulate gyri (ACG), the supramarginal gyrus, and the middle frontal gyrus in the right hemisphere. A few hubs were identified only in the low schizotypy group, including left superior occipital gyri, the left ACG, the left middle occipital gyrus (MOG), and the right cuneus (CUN). On the other hand, brain regions, including bilateral angular gyrus, the superior frontal gyrus (medial) (SFGmed), the right superior frontal gyrus (medial orbital), the left STG, and the supramarginal gyrus, were identified as hubs only in the high schizotypy group. The results are shown in **Table 2** and **Figure 4**. Further group comparisons on the mean nodal degrees of each hub that differ between 2 groups were conducted. The significant differences were found on the hubs of bilateral SFGmed (left:  $F = 5.30$ ,  $P < .05$ , partial eta square = 0.075; right:  $F = 5.02$ ,  $P < .05$ , partial eta square = 0.072), left MOG ( $F = 4.14$ ,  $P < .05$ , partial eta square = 0.060), and right CUN ( $F = 5.28$ ,  $P < .05$ , partial eta square = 0.075) (see **Figure 5**).

#### Functional Connectivity of the Abnormal GM Clusters

We conducted voxel-based analysis to examine the functional connectivity between 4 clusters as seeds, including the insula, the dIPFC, the declive of the cerebellum, the right MTG, and all other voxels in the brain controlling for age and gender. After AlphaSim correction, the high schizotypy group showed decreased functional connectivity between the left insula and the left putamen ( $t = 4.61$ , cluster size = 25, MNI coordinates: -21, 3, -15) relative to the low schizotypy group. We also found an increased functional connectivity between the left cerebellum (declive) and the right medial frontal gyrus, (BA 6,  $t = 4.25$ , cluster size = 42, MNI coordinates: 12, 12, 48) in the high schizotypy group. The results are illustrated in **Figure 6**.

#### Partial Correlations Between the SPQ Scores and Brain Structural/Functional Changes in High Schizotypy

On the brain structural changes, we found a significant positive correlation between the cognitive-perceptual scores of the SPQ and the density of right pMTG (BA 39) ( $r = .39$ ,  $P < .05$ ). On the brain functional changes, no significant correlations were found between the SPQ scores and network properties ( $C_p$ ,  $E_{loc}$ ) or mean nodal degree.

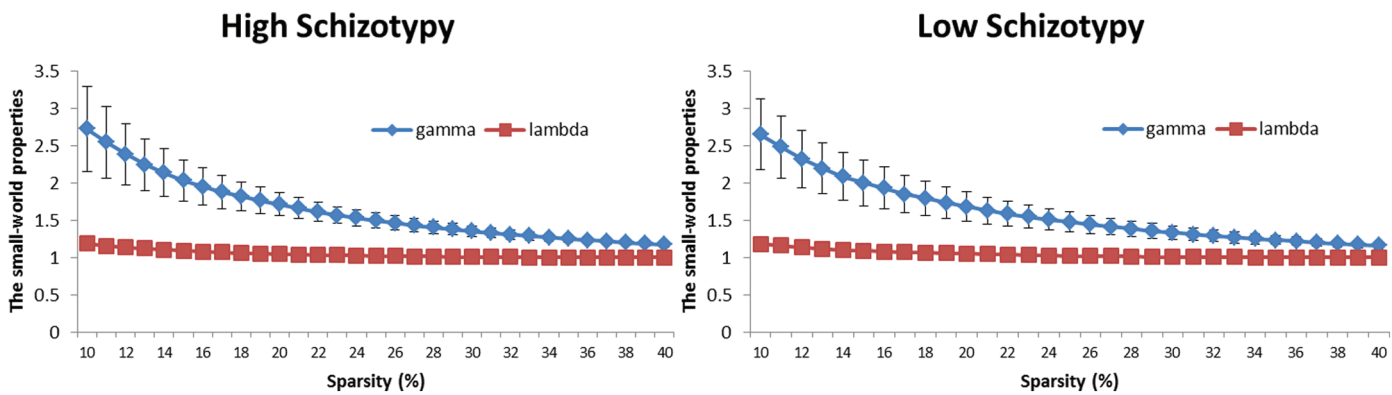


**Fig. 2.** The small-world properties in both the high schizotypy and the low schizotypy groups. Over the range of sparsity from 10% to 40%, the normalized clustering coefficient ( $\gamma$ ) and the normalized shortest path length ( $\lambda$ ) were shown for both the high and the low schizotypy groups.

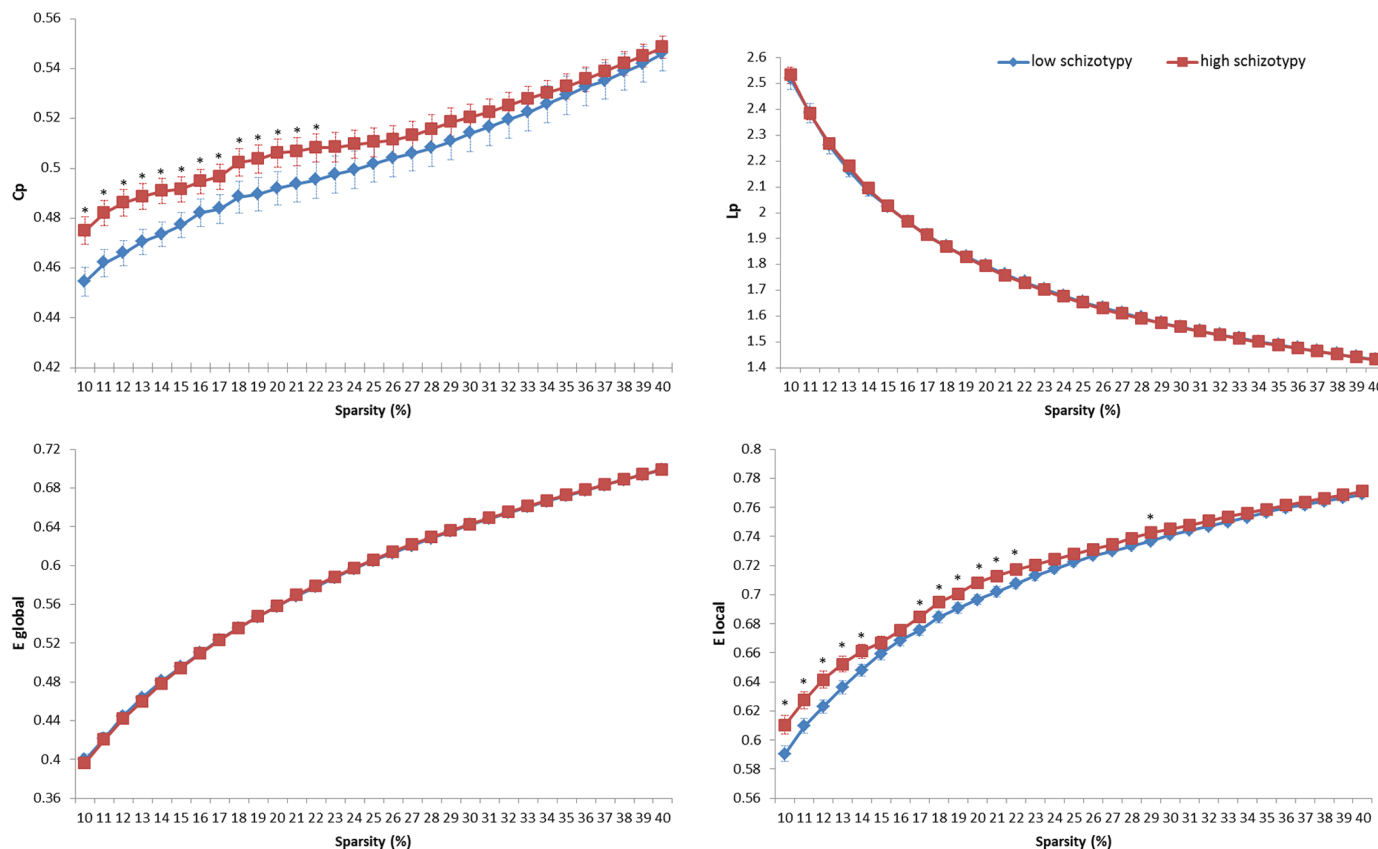


**Fig. 3.** Global network properties in both the high schizotypy and the low schizotypy groups.  $C$ : clustering coefficient;  $L_p$ : shortest path length;  $E_{\text{global}}$ : global efficiency;  $E_{\text{local}}$ : local efficiency. The group mean and standard error of the mean of the network parameter was plotted. A black asterisk (\*) indicate the difference between 2 groups is significant ( $P < .05$ , Bonferroni corrected).

## Discussion

The current study examined the morphometric abnormalities in individuals with high schizotypy, as well as the properties of resting-state functional network assessed using graph theory analysis. The main findings are summarized as below: Firstly, compared with the low schizotypy group, we found a reduction of GM density in the high schizotypy

group at the dlPFC and the insula in the left hemisphere. We also found increased GM density in the high schizotypy group in the right posterior MTG and the left cerebellum (declive). The density of the cluster in right posterior MTG was positively correlated to the cognitive-perceptual subscale scores of the SPQ. Secondly, in terms of the global and nodal characteristics of resting-state functional networks, individuals with high schizotypy showed

**Table 2.** The Hubs of the Functional Networks in Both High and Low Schizotypy Groups

Node	Normalized Nodal Degree		Regions
	High Schizotypy	Low Schizotypy	
INS.R	1.79	2.26	Insula
INS.L	1.53	2.03	Insula
ROL.R	1.59	1.69	Rolandic operculum
LING.R	1.22	1.51	Lingual gyrus
LING.L	1.20	1.49	Lingual gyrus
SMG.R	1.77	1.42	Supramarginal gyrus
ROL.L	1.66	1.36	Rolandic operculum
PoCG.R	1.80	1.31	Postcentral gyrus
PoCG.L	1.21	1.23	Postcentral gyrus
ACG.R	1.36	1.20	Anterior cingulate and paracingulate gyri
SOG.L	—	1.17	Superior occipital gyrus
ACG.L	—	1.17	Anterior cingulate and paracingulate gyri
CUN.R	—	1.12	Cuneus
MFG.R	1.45	1.12	Middle frontal gyrus
MOGL	—	1.03	Middle occipital gyrus
SFGmed.R	1.92	—	Superior frontal gyrus, medial
ANG.R	1.17	—	Angular gyrus
STG.L	1.03	—	Superior temporal gyrus
SFGmed.L	1.71	—	Superior frontal gyrus, medial
ORBsupmed.R	1.23	—	Superior frontal gyrus, medial orbital
SMG.L	1.02	—	Supramarginal gyrus
ANG.L	1.26	—	Angular gyrus

higher clustering coefficient ( $C_p$ ) and local efficiency ( $E_{loc}$ ) than low schizotypy individuals. Thirdly, several hubs of the network were identified in both groups, including the insula, the lingual gyrus, the postcentral gyrus, and the rolandic operculum. More regions in the occipital lobe were identified as hubs in the low schizotypy group, while more regions in the frontal lobe were identified as hubs in the high schizotypy group. Lastly, individuals with high schizotypy showed weaker functional connectivity between the left insula and the putamen, but stronger connectivity between the cerebellum and the medial frontal gyrus.

By far, the most consistent finding of brain structural studies has been reported in patients with schizophrenia is the reduction of GM volume or density. MRI studies in schizophrenia patients have found that the most consistent results on GM volumetric reduction are located in the temporal and frontal lobe.<sup>35</sup> Recently, an activation likelihood estimation meta-analysis study also demonstrated GM abnormality in frontal-temporal regions in first-episode and chronic patients with schizophrenia.<sup>36</sup> A longitudinal study in individuals with ultra-high-risk (UHR) state for psychosis found that structural abnormalities at the insular cortex may reflect the vulnerability for the development of psychosis,<sup>37</sup> and these UHR individuals are partly identified based on the presence of schizotypal features. In their study, individuals with UHR who developed psychosis later showed a 5% reduction per year of bilateral insular cortical GM, which was

greater than healthy controls (0.4% per year) and individuals with UHR who did not develop psychosis (0.6% per year). In the present study, we found that individuals with high schizotypy showed GM density reduction at the left insula, which is consistent with previous findings and further suggested that even in individuals from the general population who reported more psychotic-like experiences, GM reduction at the left insula may still be a potential indicator for the high-risk state. This finding may be helpful in the early detection of the high-risk population. In the present study, the dlPFC was another region which showed GM reduction in individuals with high schizotypy. This is consistent with prior studies in individuals with schizophrenia spectrum disorders,<sup>16,38</sup> as well as the finding of prefrontal changes observed in those UHR individuals converting to psychosis.<sup>39</sup> Using psychometric measures, the associations between increased self-reported schizotypal score and reduced GM volume at the prefrontal cortex has also been found.<sup>17</sup> Recently, a few studies have reported associations between schizotypy and brain structures,<sup>18,20</sup> which are different from the findings in schizophrenia patients. In addition to increased whole-brain volumes<sup>18</sup> and increased cortical thickness at the prefrontal cortex,<sup>20</sup> the higher GM density at the temporal lobe and the cerebellum in the present study might provide more evidence for potential protective or compensatory mechanisms for this high-risk population. The modulating role of dopamine

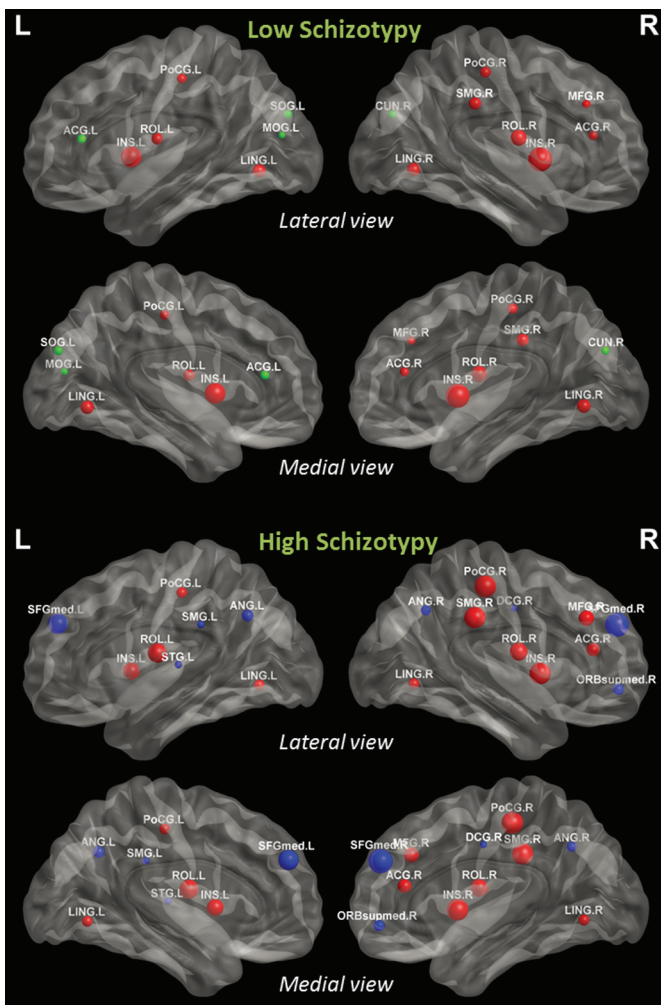


**Fig. 4.** Hub regions identified by nodal degree in the low and the high schizotypy groups. The node was identified as a hub if its normalized nodal degree was higher than the sum of the mean and SD of all nodes of the network. The size of the node shows the relative nodal degree; nodes in red indicated the common hub regions identified in 2 groups; nodes in green indicate hubs identified only in the low schizotypy group; nodes in blue indicate hubs identified only in the high schizotypy group.

and schizophrenia-like thought has been examined in healthy participants and their findings indicate a relation between positive schizotypy and hyperdopaminergia in right hemisphere.<sup>40–42</sup> We also found a significant correlation between SPQ cognitive-perceptual scores and GM density of right posterior MTG. There might be specific compensates through dopamine modulates in right hemisphere related to positive schizotypy. Taken together, the protective mechanisms have been speculated for both schizotypy and patients with schizotypal personality disorder,<sup>3</sup> suggesting that exploring the neurobiology of “resilience” warrants further investigation.<sup>43</sup>

Previous studies have suggested that the resting-state functional network in healthy controls showed small-world properties, which means higher cluster coefficients and similar path lengths, compared with random

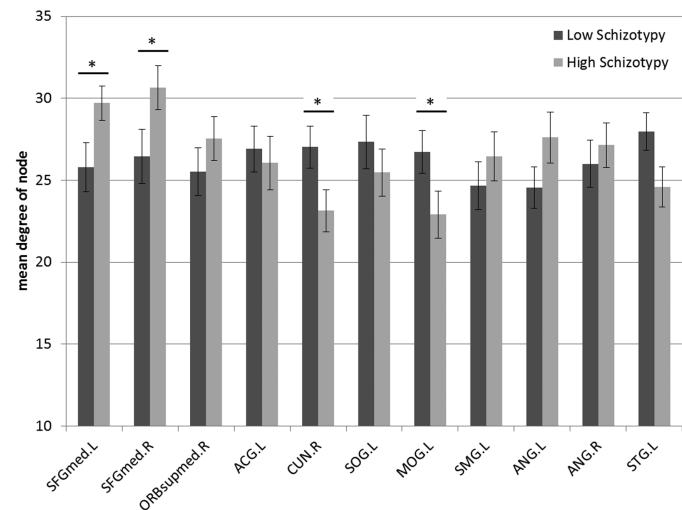


**Fig. 5.** The group comparisons on the mean nodal degree of the hubs between 2 groups. The significant differences were found on the hubs of bilateral SFGmed, left MOG, and right CUN. SFGmed: superior frontal gyrus (medial); ORBsupmed: superior frontal gyrus (medial orbital); ACG: anterior cingulate and paracingulate gyri; CUN: cuneus; SOG: superior occipital gyrus; MOG: middle occipital gyrus; SMG: supramarginal gyrus; ANG: angular gyrus; STG: superior temporal gyrus. L: left; R: right. Group comparisons on the mean nodal degree were conducted with age and gender as covariates and the threshold was set at  $P < .05$ .

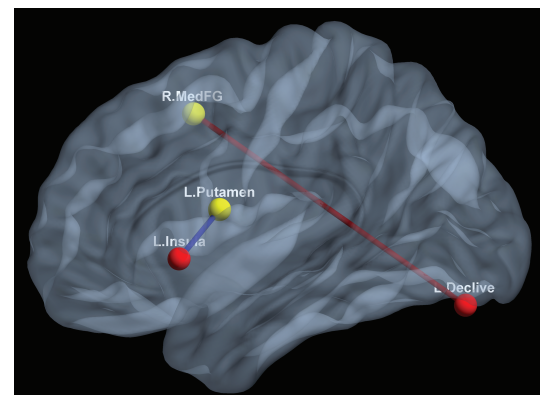


**Fig. 6.** The abnormal functional connectivity in the high schizotypy group. Compared with the low schizotypy group, individuals with high schizotypy showed decreased functional connectivity between left insula and left putamen (blue line in the figure), and hyperconnectivity between left cerebellum (declive) and right medial frontal gyrus (red line). The threshold was set at  $P < .05$  with AlphaSim correction for multiple comparisons.

networks. In patients with schizophrenia, disrupted small-world networks have been observed.<sup>23,44</sup> However, to the best of our knowledge, no other published study has examined functional connectivity using graph theoretical analysis in schizotypy individuals. In the present study, we found similar topological properties between the high schizotypy and the low schizotypy groups at both global and regional levels. This makes sense since all of our participants were recruited from college and had normal functioning at the time of testing. The relatively intact

network characteristics are consistent with the subthreshold nature of psychotic symptoms in high schizotypy individuals. Among all the small-world properties, the high schizotypy group only showed a higher local efficiency than the low schizotypy group. In terms of local efficiency, previous studies in schizophrenia showed inconsistent results. For example, Liu et al<sup>23</sup> found a lower local efficiency in 31 schizophrenia patients with a mean age of 24 years ( $SD = 6$ ) than healthy controls. However, another study found a higher local efficiency in 19 schizophrenia patients with a mean age of 36.5 years ( $SD = 11.1$ ).<sup>44</sup> This inconsistency might be attributed to the clinical heterogeneity and differences in duration of illness and warrants further exploration, especially in high-risk populations, relatives, and medication-naïve first-episode patients. Using the nodal degree, we identified the hubs of resting functional networks respectively in the high schizotypy and the low schizotypy groups. The common regions in both groups included bilateral insula, the lingual gyrus, the rolandic operculum, the postcentral gyrus, and some frontal regions, which is consistent with previous studies.<sup>32,45</sup> In contrast to the low schizotypy group, more hubs in the frontal lobe and fewer hubs in the occipital lobe were identified in individuals with high schizotypy. This indicates that the frontal lobe is more highly connected with the other regions in the whole-brain network in the high schizotypy group. Previous fMRI study using theory of mind tasks found increased activation at the prefrontal cortex in individuals with high scores on the CAPE questionnaire.<sup>46</sup> A review also found that no study had indicated a brain activation reduction at the frontal lobe, although fMRI studies found similar abnormal brain activity in schizotypy individuals as in schizophrenia patients. One possible explanation may be related to non-linear development of different brain regions in childhood and adolescent.<sup>47</sup> A longitudinal MRI study has shown that GM increases during preadolescence with a peak at around 11–12 years of age, and then decreases during postadolescence.<sup>48</sup> Compared with the low schizotypy group, the hyperconnectivity at the frontal lobe in the high schizotypy group may indicate immature brain development. Another explanation may take this hyperconnectivity as a protective factor in high schizotypy individuals that helps to maintain relatively normal behavioral performance. The trajectory of changes of structural and functional connectivity of the frontal lobes in high-risk populations need to be systematically examined across adolescent development and in relation to symptoms.<sup>49</sup>

Previous studies have found abnormal functional connectivity within the corticostriatal circuits in schizophrenia patients,<sup>50</sup> as well as between the striatal region and the insula in people at UHR for psychosis.<sup>51</sup> Consistent coactivation of the insula and the putamen has been found by a meta-analysis based on positron emission tomography and fMRI studies.<sup>52</sup> It has also been suggested that these 2 regions may play a role in the so-called

“hate circuit,” since both are activated while participants were presented with pictures of people they hated.<sup>53</sup> As a part of the dorsal striatum, it has been theorized that the putamen may be involved in the perception of contempt and disgust,<sup>54,55</sup> while the insular cortex, in particular its most anterior portion, is considered a limbic-related cortex involved in the experience of several basic emotions<sup>56</sup> and emotion regulation.<sup>57</sup> Behavioral studies have suggested that individuals with high schizotypy showed a higher level of negative emotional experience, abnormal expression, and emotional dysregulation.<sup>4</sup> In addition, the insula was also considered to relate to the somatic sensation, the deficit of which has been found in schizophrenia patients.<sup>58</sup> The weaker connection between the insula and the putamen in the high schizotypy group found in the present study may be associated with poor emotional processing and somatic sensation. In contrast, we also observed increased connectivity between the cerebellum and the medial frontal gyrus (BA 6) in high schizotypy individuals. Frontocerebellar connection plays an important role in cognitive processing such as self-reference<sup>59</sup> and conscious awareness.<sup>60</sup> A reduced association of this connection has been observed in schizophrenia patients and their siblings.<sup>61,62</sup> It remains unclear why schizotypy individuals exhibited enhanced connectivity between the medial frontal gyrus and the cerebellum. One possible explanation is that schizotypy individuals exhibit ideas of reference and are relatively sensitive to failure, defeat, and negative reactions from others, which might contribute to the hyperconnectivity between the cerebellum and the medial frontal gyrus.

The present study is unique in our integration of brain structural and functional connectivity to illustrate the brain alteration in individuals with schizotypy. Based on the examination of the brain GM/WM density and resting-state functional connectivity, we further took the clusters which presented abnormal GM density as ROIs to explore their potential functional disconnection, which could contribute to the understanding of the neural correlates of schizotypy. However, there are several limitations in the present study. Firstly, we only adopted a self-reported measure for schizotypy. Using a structural interview would be more accurate and reliable in recruiting appropriate participants in future studies. Secondly, since we did not have specific behavioral tasks capturing emotional processing or prefrontal functions, we could only speculate on the underlying associations with brain alteration based on findings from previous studies. These speculations need to be tested in future studies by adopting more specific paradigms or tasks. Thirdly, since the present study was conducted in relatively well-functioning college students and was exploratory in nature, we used the AlphaSim correction for multiple comparisons in our study. Fourth, the depression and anxiety were not been controlled in the present study, which should be considered in the future studies. The latest evidence showed

that individuals with different subtypes of schizotypy may have unique performance on emotional and cognitive tasks. Future studies should consider the different dimensions of schizotypy.

In conclusion, by integrating brain structural morphometric analysis and graph theory-based network analysis, our findings suggest that the individuals with high schizotypy already exhibit some abnormalities in terms of GM and resting-state functional connectivity, especially in the frontal lobe.

## Funding

“Strategic Priority Research Program (B)” of the Chinese Academy of Sciences (XDB02030002); the National Science Fund China (81088001, 91132701); Knowledge Innovation Project of the Chinese Academy of Sciences (KSCX2-EW-J-8). C.P. was supported by a NHMRC Senior Principal Research Fellowship (ID: 628386) and NARSAD Distinguished Investigator Award.

## Acknowledgments

The authors have declared that there are no conflicts of interest in relation to the subject of this study.

## References

- Nelson MT, Seal ML, Pantelis C, Phillips LJ. Evidence of a dimensional relationship between schizotypy and schizophrenia: a systematic review. *Neurosci Biobehav Rev*. 2013;37:317–327.
- Battaglia M, Cavallini MC, Macciardi F, Bellodi L. The structure of DSM-III-R schizotypal personality disorder diagnosed by direct interviews. *Schizophr Bull*. 1997;23:83–92.
- Ettinger U, Meyhöfer I, Steffens M, Wagner M, Koutsouleris N. Genetics, cognition, and neurobiology of schizotypal personality: a review of the overlap with schizophrenia. *Front Psychiatry*. 2014;5:18.
- Phillips LK, Seidman LJ. Emotion processing in persons at risk for schizophrenia. *Schizophr Bull*. 2008;34:888–903.
- American Psychiatric Association. *Diagnostic and Statistical Manual of Mental Disorders (4th ed, text revision) (DSM-IV-TR)*. Washington, DC: American Psychiatric Association; 2000.
- Kendler KS. Diagnostic approaches to schizotypal personality disorder: a historical perspective. *Schizophr Bull*. 1985;11:538–553.
- Raine A. The SPQ: a scale for the assessment of schizotypal personality based on DSM-III-R criteria. *Schizophr Bull*. 1991;17:555–564.
- Chapman LJ, Chapman JP, Raulin ML. Body-image aberration in Schizophrenia. *J Abnorm Psychol*. 1978;87:399–407.
- Chapman LJ, Chapman JP, Raulin ML. Scales for physical and social anhedonia. *J Abnorm Psychol*. 1976;85:374–382.
- Eckblad M, Chapman LJ. Magical ideation as an indicator of schizotypy. *J Consult Clin Psychol*. 1983;51:215–225.
- Dickey CC, McCarley RW, Shenton ME. The brain in schizotypal personality disorder: a review of structural MRI and CT findings. *Harv Rev Psychiatry*. 2002;10:1–15.
- Dickey CC, McCarley RW, Voglmaier MM, et al. Schizotypal personality disorder and MRI abnormalities of temporal lobe gray matter. *Biol Psychiatry*. 1999;45:1393–1402.
- Kawasaki Y, Suzuki M, Nohara S, et al. Structural brain differences in patients with schizophrenia and schizotypal disorder demonstrated by voxel-based morphometry. *Eur Arch Psychiatry Clin Neurosci*. 2004;254:406–414.
- Koo MS, Levitt JJ, McCarley RW, et al. Reduction of caudate nucleus volumes in neuroleptic-naïve female subjects with schizotypal personality disorder. *Biol Psychiatry*. 2006;60:40–48.
- Dickey CC, McCarley RW, Voglmaier MM, et al. A MRI study of fusiform gyrus in schizotypal personality disorder. *Schizophr Res*. 2003;64:35–39.
- Asami T, Whitford TJ, Bouix S, et al. Globally and locally reduced MRI gray matter volumes in neuroleptic-naïve men with schizotypal personality disorder: association with negative symptoms. *JAMA Psychiatry*. 2013;70:361–372.
- Ettinger U, Williams SC, Meisenzahl EM, Möller HJ, Kumari V, Koutsouleris N. Association between brain structure and psychometric schizotypy in healthy individuals. *World J Biol Psychiatry*. 2012;13:544–549.
- Modinos G, Mechelli A, Ormel J, Groenewold NA, Aleman A, McGuire PK. Schizotypy and brain structure: a voxel-based morphometry study. *Psychol Med*. 2010;40:1423–1431.
- Nelson MT, Seal ML, Phillips LJ, Merritt AH, Wilson R, Pantelis C. An investigation of the relationship between cortical connectivity and schizotypy in the general population. *J Nerv Ment Dis*. 2011;199:348–353.
- Kühn S, Schubert F, Gallinat J. Higher prefrontal cortical thickness in high schizotypal personality trait. *J Psychiatr Res*. 2012;46:960–965.
- Williamson PC, Allman JM. A framework for interpreting functional networks in schizophrenia. *Front Hum Neurosci*. 2012;6:184.
- Bullmore E, Sporns O. Complex brain networks: graph theoretical analysis of structural and functional systems. *Nat Rev Neurosci*. 2009;10:186–198.
- Liu Y, Liang M, Zhou Y, et al. Disrupted small-world networks in schizophrenia. *Brain*. 2008;131:945–961.
- Lagioia A, Van De Ville D, Debbané M, Lazeyras F, Eliez S. Adolescent resting state networks and their associations with schizotypal trait expression. *Front Syst Neurosci*. 2010;4:pii.
- Chen WJ, Hsiao CK, Lin CC. Schizotypy in community samples: the three-factor structure and correlation with sustained attention. *J Abnorm Psychol*. 1997;106:649–654.
- Annett M. A classification of hand preference by association analysis. *Br J Psychol*. 1970;61:303–321.
- Gong YX, Dai XY. Application of the short forms of Wechsler Intelligence Scale. *J Cent South Univ (Med Sci)*. 1984;4:393–400.
- Ashburner J. A fast diffeomorphic image registration algorithm. *NeuroImage*. 2007;38:95–113.
- Chao-Gan Y, Yu-Feng Z. DPARSF: A MATLAB Toolbox for “Pipeline” Data Analysis of Resting-State fMRI. *Front Syst Neurosci*. 2010;4:13.
- Tzourio-Mazoyer N, Landau B, Papathanassiou D, et al. Automated anatomical labeling of activations in SPM using a macroscopic anatomical parcellation of the MNI MRI single-subject brain. *Neuroimage*. 2002;15:273–289.

31. Achard S, Bullmore E. Efficiency and cost of economical brain functional networks. *PLoS Comput Biol.* 2007;3:e17.
32. Tian L, Wang J, Yan C, He Y. Hemisphere- and gender-related differences in small-world brain networks: a resting-state functional MRI study. *Neuroimage.* 2011;54:191–202.
33. Brett M, Anton J-L, Valabregue R, Poline J-B. Region of interest analysis using the MarsBar toolbox for SPM 99. *NeuroImage.* 2002;16:S497.
34. Song XW, Dong ZY, Long XY, et al. REST: a toolkit for resting-state functional magnetic resonance imaging data processing. *PLoS One.* 2011;6:e25031.
35. Shenton ME, Dickey CC, Frumin M, McCarley RW. A review of MRI findings in schizophrenia. *Schizophr Res.* 2001;49:1–52.
36. Chan RC, Di X, McAlonan GM, Gong QY. Brain anatomical abnormalities in high-risk individuals, first-episode, and chronic schizophrenia: an activation likelihood estimation meta-analysis of illness progression. *Schizophr Bull.* 2011;37:177–188.
37. Takahashi T, Wood SJ, Yung AR, et al. Insular cortex gray matter changes in individuals at ultra-high-risk of developing psychosis. *Schizophr Res.* 2009;111:94–102.
38. Raine A, Lencz T, Yaralian P, et al. Prefrontal structural and functional deficits in schizotypal personality disorder. *Schizophr Bull.* 2002;28:501–513.
39. Sun D, Phillips L, Velakoulis D, et al. Progressive brain structural changes mapped as psychosis develops in ‘at risk’ individuals. *Schizophr Res.* 2009;108:85–92.
40. Krummenacher P, Landis T, Sandor PS, Fathi M, Brugger P. Psychometric schizotypy modulates levodopa effects on lateralized lexical decision performance. *J Psychiatr Res.* 2005;39:241–250.
41. Mohr C, Landis T, Sandor PS, Fathi M, Brugger P. Nonstereotyped responding in positive schizotypy after a single dose of levodopa. *Neuropsychopharmacology.* 2004;29:1741–1751.
42. Mohr C, Landis T, Bracha HS, Fathi M, Brugger P. Levodopa reverses gait asymmetries related to anhedonia and magical ideation. *Eur Arch Psychiatry Clin Neurosci.* 2005;255:33–39.
43. Pantelis C, Bartholomeusz CF. Social neuroscience in psychiatry: pathways to discovering neurobiological risk and resilience. *World Psychiatry.* 2014;13:146–147.
44. Yu Q, Sui J, Rachakonda S, et al. Altered topological properties of functional network connectivity in schizophrenia during resting state: a small-world brain network study. *PLoS One.* 2011;6:e25423.
45. Melie-García L, Sanabria-Díaz G, Sánchez-Catasús C. Studying the topological organization of the cerebral blood flow fluctuations in resting state. *Neuroimage.* 2013;64:173–184.
46. Modinos G, Renken R, Shamay-Tsoory SG, Ormel J, Aleman A. Neurobiological correlates of theory of mind in psychosis proneness. *Neuropsychologia.* 2010;48:3715–3724.
47. Blakemore SJ, Choudhury S. Development of the adolescent brain: implications for executive function and social cognition. *J Child Psychol Psychiatry.* 2006;47:296–312.
48. Giedd JN, Blumenthal J, Jeffries NO, et al. Brain development during childhood and adolescence: a longitudinal MRI study. *Nat Neurosci.* 1999;2:861–863.
49. Cropley VL, Pantelis C. Using longitudinal imaging to map the ‘relapse signature’ of schizophrenia and other psychoses. *Epidemiol Psychiatr Sci.* 2014;23:219–225.
50. Tu PC, Hsieh JC, Li CT, Bai YM, Su TP. Cortico-striatal disconnection within the cingulo-opercular network in schizophrenia revealed by intrinsic functional connectivity analysis: a resting fMRI study. *Neuroimage.* 2012;59:238–247.
51. Dandash O, Fornito A, Lee J, et al. Altered striatal functional connectivity in subjects with an at-risk mental state for psychosis. *Schizophr Bull.* 2014;40:904–913.
52. Postuma RB, Dagher A. Basal ganglia functional connectivity based on a meta-analysis of 126 positron emission tomography and functional magnetic resonance imaging publications. *Cereb Cortex.* 2006;16:1508–1521.
53. Zeki S, Romaya JP. Neural correlates of hate. *PLoS One.* 2008;3:e3556.
54. Calder AJ, Keane J, Manes F, Antoun N, Young AW. Impaired recognition and experience of disgust following brain injury. *Nat Neurosci.* 2000;3:1077–1078.
55. Phillips ML, Young AW, Senior C, et al. A specific neural substrate for perceiving facial expressions of disgust. *Nature.* 1997;389:495–498.
56. Phan KL, Wager T, Taylor SF, Liberzon I. Functional neuroanatomy of emotion: a meta-analysis of emotion activation studies in PET and fMRI. *Neuroimage.* 2002;16:331–348.
57. Goldin PR, McRae K, Ramel W, Gross JJ. The neural bases of emotion regulation: reappraisal and suppression of negative emotion. *Biol Psychiatry.* 2008;63:577–586.
58. Wyllie KP, Tregellas JR. The role of the insula in schizophrenia. *Schizophr Res.* 2010;123:93–104.
59. Gusnard DA, Raichle ME, Raichle ME. Searching for a baseline: functional imaging and the resting human brain. *Nat Rev Neurosci.* 2001;2:685–694.
60. Horovitz SG, Braun AR, Carr WS, et al. Decoupling of the brain’s default mode network during deep sleep. *Proc Natl Acad Sci USA.* 2009;106:11376–11381.
61. Collin G, Hulshoff Pol HE, Hajcma SV, Cahn W, Kahn RS, van den Heuvel MP. Impaired cerebellar functional connectivity in schizophrenia patients and their healthy siblings. *Front Psychiatry.* 2011;2:73.
62. Park KM, Kim JJ, Seok JH, Chun JW, Park HJ, Lee JD. Anhedonia and ambivalence in schizophrenic patients with fronto-cerebellar metabolic abnormalities: a fluoro-d-glucose positron emission tomography study. *Psychiatry Investig.* 2009;6:72–77.